Thermally stimulated luminescence and conductivity of doped Ar solids

1996 J. Phys.: Condens. Matter 8 3677

(http://iopscience.iop.org/0953-8984/8/20/014)

J. Phys.: Condens. Matter **8** (1996) 3677–3689. Printed in the UK

Thermally stimulated luminescence and conductivity of doped Ar solids

A Schrimpf†, C Boekstiegel‡, H-J Stöckmann†, T Bornemann†, K Ibbeken†, J Kraft† and B Herkert†

† Fachbereich Physik der Philipps-Universität Marburg and Wissenschaftliches Zentrum für Materialwissenschaften, Renthof 5, D-35032 Marburg, Germany

‡ Laboratorium für Kristallographie, ETH-Zentrum, CH-8092 Zürich, Switzerland

Received 24 July 1995, in final form 4 March 1996

Abstract. Solid Ar samples doped with the noble metal atoms Au or Ag as well as with O_2 molecules have been exposed to synchrotron and x-ray irradiation. Impurity trapping of excitons generated by the irradiation partly led to an ionization; the impurities formed deep traps for one type of charge carrier, the complementary ones were promoted into band states and subsequently captured into shallow traps. These charge carriers could be thermally released giving rise to thermally stimulated luminescence (TSL) and conductivity (TSC) signals, which were recorded simultaneously. The glow curves of both, TSL and TSC, clearly revealed the existence of intrinsic and extrinsic electron traps. Using a step-like temperature increase it could be demonstrated that traps exist with a broad distribution of binding energies. A first-order kinetics model was developed to extract binding energies from the temperature dependence of the thermally stimulated luminescence.

1. Introduction

The irradiation of a doped rare gas solid with light mainly leads to a relaxation of the excitation energy in the form of a directly following fluorescence on the emission lines of the dopants. In a small part of the relaxation processes the excitation energy is stored in shallow traps and is released upon subsequent heating giving rise to thermally stimulated luminescence (TSL). The identification of these traps often constitutes a severe problem [1]. It is one of the aims of this paper to give an identification of TSL centres found by us in synchrotron or x-ray irradiated doped rare gas solids.

The irradiations described in the literature have been either specific by exciting directly an optical transition of the dopants or unspecific by producing excitons or free charge carriers. The first type of excitation is often used in the case of molecular dopants. Fajardo *et al* observed the relaxation of optically accessed charge transfer states of halogen-doped solid xenon [2]. The halogen molecule was cracked by near UV excitation; electrons were trapped at the halogen atoms and the holes were stored in shallow traps in the Xe solid. Thermal release of the holes and subsequent recombination with the negative halogen atoms led to an exciplex emission which was observed as thermoluminescence. Danilychev *et al* studied the recombination of atomic oxygen in crystalline Kr and Xe [3]. The matrices were prepared with O_2 molecules as dopants which were cracked by excitation of a predissociative O_2 state. During thermal annealing the oxygen atoms became mobile and started to diffuse. Their recombination to O_2 molecules was accompanied by an emission of the well-known

0953-8984/96/203677+13$19.50

Herzberg bands. This so-called chemiluminescence process has been reported for a variety of molecular-doped rare gas solids (see reference [3] and references therein).

In the case of x-ray irradiation, on the other hand, direct excitation of the impurities is negligible because of the much higher number of host atoms. Here the primary absorption process is a photoeffect at the host atoms. In the subsequent deceleration of the hot photoelectrons a large number of excitons (typically several hundreds) is produced. A part of them transports the excitation energy to the dopants giving rise to their characteristic fluorescence, another part is trapped. Two earlier experiments are known to us where TSL after x-ray irradiation was studied. Dersch *et al* observed the thermoluminescence of Ag atoms embedded in solid Ar [4]. In a second paper the thermoluminescence of molecular self-trapped excitons produced in undoped solid Kr by x-ray irradiation was reported by Kirm *et al* [5]. As a selective excitation of excitons is not possible with x-rays, from these experiments one can only indirectly conclude that excitons are somehow involved in the formation of thermoluminescence centres.

Binding energies of the trapped charge carriers have been calculated by Fajardo *et al* [2] and Kirm *et al* [5] using a first-order kinetics model with a single type of trap with just one fixed binding energy. However, the last ten years of investigations in the field of spectroscopy of rare gas solids have shown that vacuum sublimed rare gas films are microcrystalline or even nanocrystalline [6, 7]. Therefore inhomogeneous distributions of trap binding energies have to be considered. Indeed, the experiments mentioned above on Ag-doped Ar samples [4] could be explained only under the assumption of broad distributions of binding energies.

The existence of self-trapped holes in rare gas solids has been established by hole-transport measurements [8] and theoretical investigations [9, 10], though the calculated binding energies are much higher than those evaluated from the transport measurements. To our knowledge so far no experimental or theoretical evidence for self-trapped electrons in Ar, Kr or Xe solids exists.

In this paper TSL and thermally stimulated conductivity (TSC) measurements on VUV-light and x-ray irradiated doped Ar samples are presented and discussed. The paper concentrates on two main points. First TSL and TSC spectra of matrices doped with impurities of different electronegativity are presented. Comparing the results from argon doped with Ag and Au atoms with electronegativities of 1.9 and 2.4 [11], respectively, and with oxygen with an electronegativity of 3.5 [11] we were able to identify indirectly intrinsic and extrinsic electron traps in solid Ar. As the experiments originally aimed at other problems (the transport of excitation energy via excitons through the rare gas solids [12, 13]), larger systematics on different dopants and rare gases are not available. We believe, however, that the existing data base is completely sufficient to come to the conclusions derived below. The second main aspect is a thorough theoretical description of thermoluminescence glow curves in the presence of an inhomogeneous distribution of activation energies. Our experiments have shown that at least in rare gas solids it is *not* sufficient to consider just a limited number of sharp excitation energies, a point mainly overlooked hitherto. A review of our experiments on electronic transport and relaxation processes in rare gas solids including some previous TSL results can be found in reference [13].

2. Experimental details

The synchrotron radiation experiments were performed with a UHV matrix isolation apparatus at the Berlin storage ring BESSY. The experimental set-up has been described

recently [12, 14], therefore only the main features are repeated here. The samples were prepared by simultaneous condensation of the metal vapour from a UHV evaporator (Omicron EFM 3) or the dopant gas and of the matrix gas onto a LiF substrate, cooled by a continuous flow cryostat (Oxford CF 1100 UHV, minimal temperature 5 K). Temperatures were measured with a calibrated carbon resistor at the sample holder. The deposition rate of the rare gas was determined interferometrically with a He–Ne laser and the metal atom deposition rate was monitored with an oscillator microbalance. Doping with O_2 was achieved by appropriately adjusted gas-flow rates of dopant gas and rare gas, respectively, into the vacuum chamber using separate metal needle valves for each gas. The dopant to rare gas ratio was varied between 10^{-5} and 10^{-2}, the residual gas contamination was smaller than 10^{-5}. Typical thicknesses were about 20 μm. If not explicitly mentioned, the samples were annealed up to 30 K for several minutes before exposure to radiation.

The synchrotron light from the storage ring was passed through a 1 m Seya monochromator. We used a 600 lines/mm grating covering an energy range from 5 eV to 25 eV and blazed at approximately 16 eV. For a part of the experiments zero-order, namely white, synchrotron radiation was used. Here the maximum energy was limited to approximately 25 eV by the coating of optical components in the beamline. The Ar excitons are ranging from 12 eV to 14 eV [15], the bandgap energy is 14.15 eV [16]. Fluorescence in the visible and the near UV spectral range was detected with an optical multi-channel detector (model 1461, EG&G) hooked onto the exit of a monochromator. Thus we were able to detect the complete fluorescence spectrum in a window of 450 nm between the limits of 180 nm (6.9 eV) and 800 nm (1.55 eV). With a 100 μm entrance slit the resolution was limited to 2 nm. Emitted light in the VUV range below 11.3 eV was passed through an evacuated 0.3 m monochromator (McPherson model 218) and detected with a solar blind multiplier. Two interlaced comb-like electrodes made of gold evaporated onto the LiF sample holder were used for conductivity measurements. Both the width of the electrodes and the separation between the electrodes were 150 μm. Two shielded cables were connected via spring contacts to the electrodes. Applying a typical voltage of 40 V to the electrodes an electrical field of approximately 2700 V cm^{-1} was obtained. With an electrometer amplifier (Keithley 617) currents in the range of 0.1 fA to 200 nA could be detected.

The set-up for x-ray irradiation of doped rare gas solids has been described in reference [4]. The aluminium sample holder was cooled by an Oxford continuous flow cryostat CF 1100. CaF_2 or LiF substrates could not be used because of the production of fluorescing colour centres by x-ray irradiation (in the synchrotron experiments the application of LiF windows posed no problems; we never observed fluorescence or TSL from the substrate). A tungsten x-ray tube (Isovolt 160, Seifert) was typically operated at 60 kV and 19 mA for sample irradiation. The emission of the doped rare gas samples in the visible and near UV spectral range was monitored with the same set-up as described above. The residual gas contamination of this system was smaller than 10^{-4}.

Spectra of TSL and TSC have been taken by applying either a linear temperature increase of 1.5 K min^{-1} or step-like temperature ramps, both of which were adjusted with the help of a programmable Oxford temperature controller ITC4.

3. Experimental results

Figure 1 shows TSL glow curves for a number of differently doped Ar samples after different irradiation conditions. The total number of photons detected in a TSL run was always of the order of several tens of thousands, corresponding to about 10^{-4} of the total

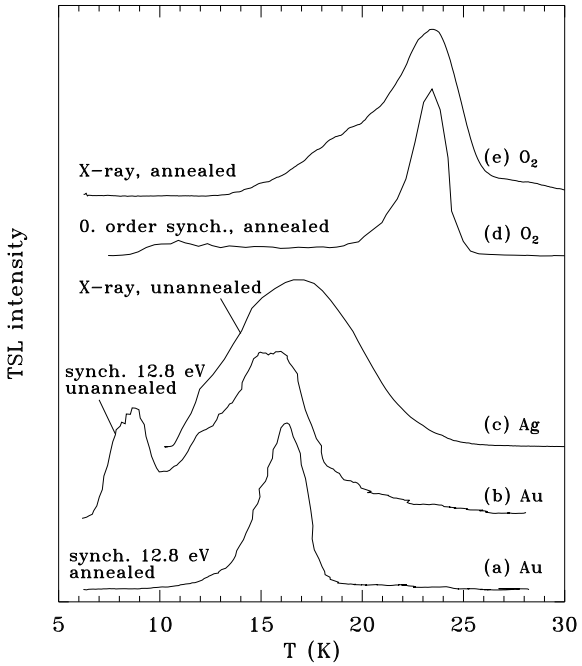

Figure 1. Glow curves of the thermally stimulated luminescence of differently doped and irradiated Ar samples: (a), Au, concentration 4×10^{-4}, annealed at 30 K, after 30 min excitation of the Ar $n = 1$ exciton with synchrotron light; (b), Au, same sample as (a), same excitation, but unannealed; (c), Ag, concentration 10^{-3}, unannealed sample, after 35 min x-ray irradiation; (d), O_2, concentration 10^{-3}, after 30 min irradiation with zero-order synchrotron light, annealed at 30 K; (e), O_2, concentration 10^{-3}, after 60 min x-ray irradiation, annealed at 30 K.

number of photons detected in the fluorescence *during* the irradiation. The two lower glow curves in figure 1 were taken of the same Au-doped Ar sample before and after annealing. Curve (b) represents the first glow curve after excitation of the Ar $n = 1$ exciton, whereas curve (a) was taken after a second exposure to synchrotron radiation at liquid He temperature. Not unexpectedly the unannealed sample shows more structure, inhomogeneous broadening as well as additional peaks. The glow curves of unannealed samples are not exactly reproducible as was also reported by other authors [2, 3]. The glow curve *after* annealing *is* reproducible, the measurement (irradiation, heating and measuring, cooling down) can be repeated several times with the same sample. For the quantitative analysis described in this paper only measurements of pre-annealed samples were used. A comparison of curve (c), which was taken of an Ag-doped Ar sample after exposure to *x-ray irradiation*, with curves (a) and (b), taken after *exciton excitation* yields another important result. The peak at about 16 K is a common feature of all our Ag- and Au-doped matrices, unannealed or annealed. It has already been found in our earlier x-ray studies [4], but with the set-up used at that time it was not possible to study directly the role of excitons during the production or population of thermoluminescence centres. With the help of the synchrotron experiments (curves (a) and (b)) it is now definitely proven that *excitons are sufficient to produce or populate thermoluminescence centres* in Au-doped rare gas crystals. Free charge carriers due to x-ray or synchrotron irradiation into the conduction band of the samples are not necessary.

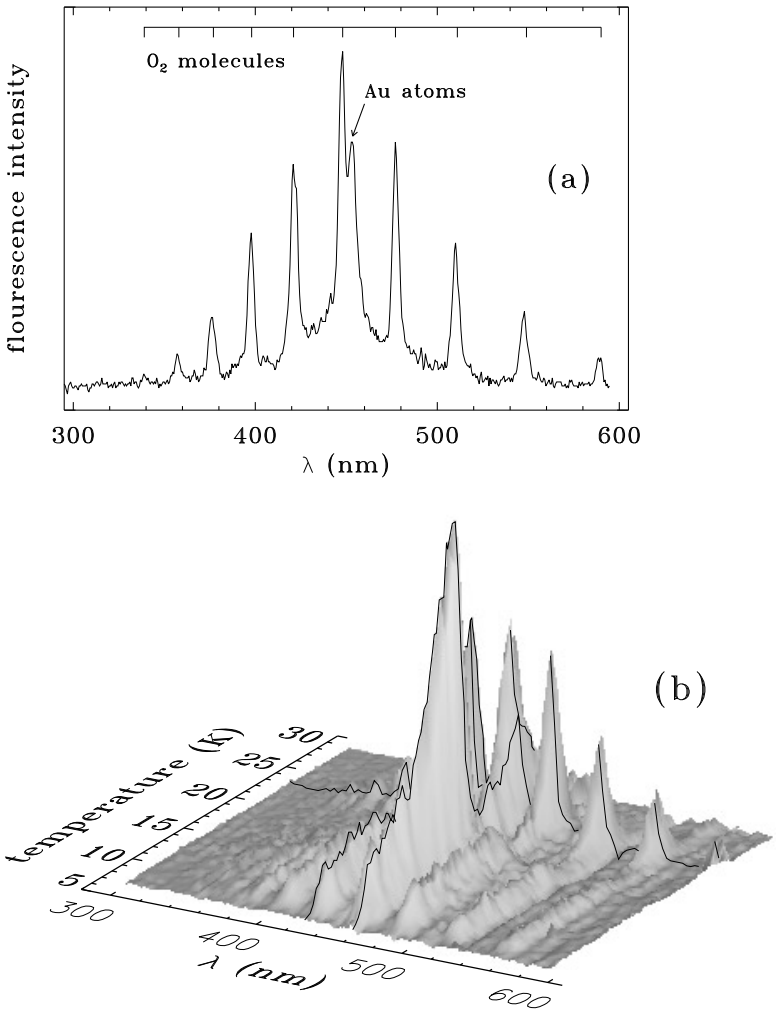

Figure 2. Thermally stimulated luminescence and conductivity of a Au- and O_2-doped Ar sample after irradiation with zero-order synchrotron light (Au concentration 8×10^{-4}, O_2 concentration approximately 10^{-5}, sample thickness 21 μm). (a) the TSL spectrum at 23 K showing the Herzberg band of O_2 and an emission of Au at 452 nm (2.74 eV) [23]. (b) A series of 150 TSL spectra showing dependence on temperature. The spectrum shown in (a) is marked by a line parallel to the wavelength axis. (c) Glow curves of the O_2 emission at 421 nm (2.95 eV), of the Au atom emission at 452 nm (2.74 eV), both marked in (b) as lines parallel to the temperature axis, and the simultaneously measured TSC signal.

The observation of a thermally stimulated current parallel to the stimulated luminescence provided further information to clarify the picture of the processes during exciton trapping and annealing. We selected an Ar sample doped with Au *and* O_2 for presentation here (figure 2, Au concentration 8×10^{-4}, O_2 concentration approximately 10^{-5}), because it is best suited to demonstrating the influence of impurities with different electronegativities on the behaviour of charge carriers. The O_2 doping was due to a contamination in the gas line and was estimated from the residual gas pressure. It has long been known that O_2 is a

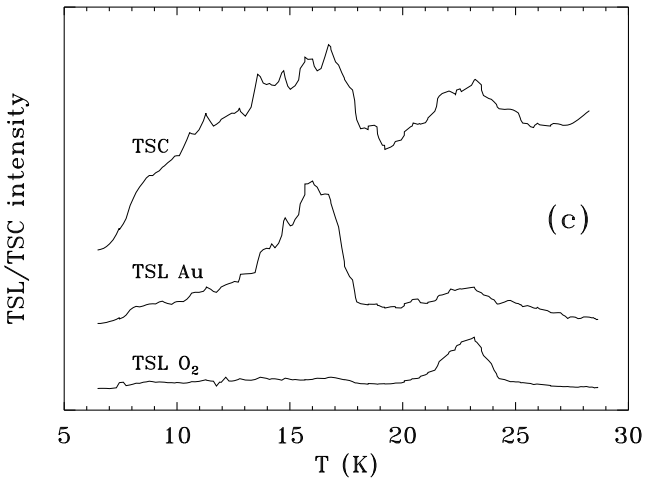

Figure 2. (Continued.)

highly efficient trap of electronic excitations in rare gas solids [17]. In the central part (b) of figure 2 thermoluminescence spectra in dependence on temperature are depicted; to get an idea of the observed fluorescence a single thermoluminescence spectrum at approximately 23 K is presented in figure 2(a), showing the O_2 Herzberg lines and the emission of Au atoms. In figure 2(c) the glow curves of one of the O_2 Herzberg lines and of the Au emission are shown together with the corresponding TSC signal.

The TSC spectrum demonstrates directly the existence of free charge carriers during the thermoluminescence process. The Au thermoluminescence at about 16 K obviously is due to a release of trapped charge carriers with subsequent radiative recombination at the Au atoms. As mentioned above we observed a peak at the same temperature in the glow curves of Ag-doped Ar samples, too (curve (c) of figure 1), but we did not find it in the glow curves of O_2 dopants (curves (d) and (e) of figure 1). The peak in the glow curve of the O_2 emission at about 23 K is caused by chemiluminescence of O_2. This was verified by the observation of an atomic oxygen emission building up during irradiation and disappearing again synchronously with the TSC at 23 K. This peak is also correlated with the release of charge carriers.

The series of thermoluminescence spectra shown in figure 2 was taken after irradiation with zero-order instead of monochromatic synchrotron light. There are two motivations for this. First, the intensity of the thermoluminescence signals is much higher, since with zero-order synchrotron light there is a much higher intensity of incoming light. Second, irradiation into one of the Ar exciton bands is not sufficient to produce significant amounts of atomic oxygen in the solid, whereas the higher-energy light (of up to 25 eV) efficiently cracks the O_2 molecules in the matrix.

The fact that the existence or nonexistence of the 16 K peak is correlated with the electronegativities of Au (2.4) and Ag (1.9) on the one hand and of O (3.5) on the other allows one to propose a model for the nature of the charge carrier traps. As the electronegativity of O is very high, oxygen atoms certainly serve as *extrinsic electron* traps. Thus the appearance of free charge carriers during the O_2 chemiluminescence can be explained by a recombination of O^- ions with neutral O atoms and a release of the bound electrons. On the other hand Ag and Au atoms are more likely to form hole traps, that

is, they will be ionized to Au^+ and Ag^+ by the exciton trapping process while the free electron has to be captured in an electron trap. The 16 K peak in the Au and Ag glow curves is independent of the impurity and is absent in the thermoluminescence of O_2 in solid Ar samples; therefore this peak at 16 K must be due to a release of electrons from *intrinsic electron* traps.

There is an additional observation that corroborates the picture that O and Au atoms serve as extrinsic electron and hole traps, respectively. The spectrum of figure 2(a), taken at about 23 K, shows emission by O_2 molecules and Au atoms simultaneously. The emission by Au atoms at 23 K does not show up without the presence of oxygen atoms (see curves (a) and (b) in figure 1); also the TSC peak at 23 K does not show up without oxygen atoms in the matrix. So here (at about 23 K) electrons are released from the O^- ions acting as extrinsic electron traps which subsequently can recombine with the holes trapped at the Au atoms giving rise to the characteristic Au emission.

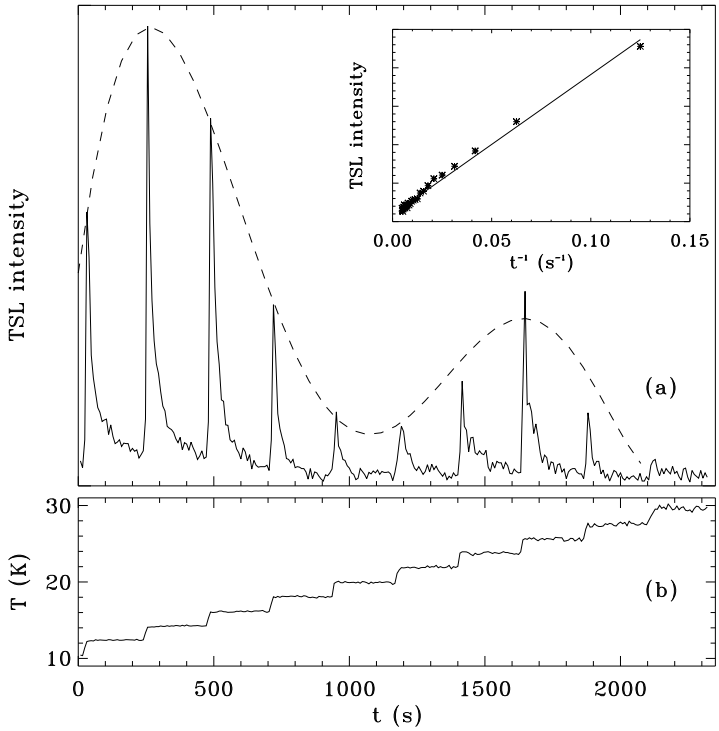

Figure 3. (a) The TSL of a Au-doped Ar sample after x-ray irradiation (Au concentration 10^{-3}, sample thickness 13 μm, irradiation time 1 h) as a function of time. In the inset the intensity of the highest of the TSL peaks is plotted versus t^{-1}. (b) Temperature as a function of time.

We now turn to the discussion of the binding energies of the charge carrier traps. In reference [4] Dersch *et al* concluded from a more qualitative measurement that it is necessary to consider a distribution of traps with different binding energies. As mentioned in the introduction one purpose of this paper is to discuss this problem *quantitatively*. In figure 3 we present a measurement that clearly shows that one has to take into account large inhomogeneous distributions. The thermoluminescence of an x-ray irradiated Au-doped Ar matrix was investigated using a step-like temperature scan. Each temperature step is followed by a renewed TSL flash and the thermoluminescence decreases almost

down to the noise level before the next temperature step. This measurement shows unambiguously that there is a distribution of traps with different activation energies which are sequentially emptied. With a linear temperature ramp one would have observed a glow curve corresponding to the envelope of the spikes (dashed line in figure 3) like the one in figure 2(c). This shows that a linear temperature ramp is not suited to determining whether there is a broad distribution of trap energies or whether there are just two types of traps with well-defined energies. In the inset in figure 3(a) the TSL intensity of the second temperature step is plotted as a function of the reciprocal time t; the TSL intensity does not show an exponential decrease, which is what would be expected for a single trap, but decreases with t^{-1}. This is exactly what is expected if the distribution of binding energies is homogeneous over the energy range probed within one temperature step (see section 4).

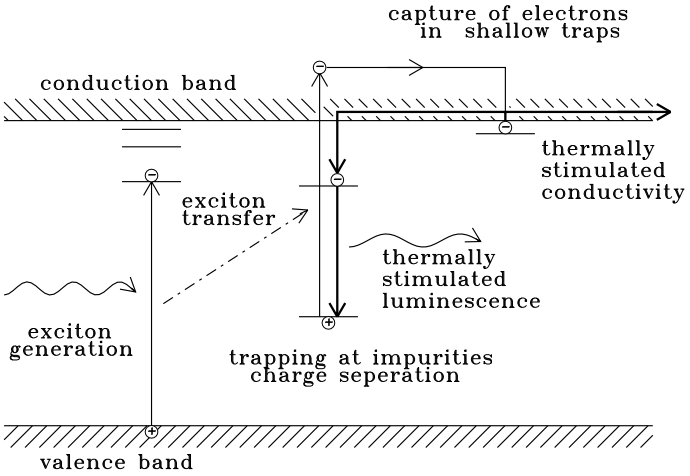

Figure 4. The model for the observed thermally stimulated processes.

4. Theoretical interpretation

Our model is sketched in figure 4. First, excitons are generated, either directly via absorption or indirectly via thermalization of high-energy photoelectrons being produced by x-ray irradiation. Then the excitons transfer their excitation energy to the impurities, which partly are ionized during the trapping process. In figure 4 it is assumed that the electrons are captured in shallow intrinsic traps whereas the holes are trapped in deep impurity states. In principle the roles of electrons and holes are interchangeable, the experiment cannot discriminate between the two alternatives. If during annealing there is enough thermal energy to release the charge carriers they can either recombine with their counterparts at the impurities with the subsequent emission of light or can be detected via a thermally stimulated current.

The temperature dependence of the thermoluminescence intensity contains the information on the distribution of trap binding energies. It is the aim of this section to establish a relation between these two quantities. For the moment we start with the simplest of all possible models and assume that there is only one type of electron trap with binding energy E. The numbers of charge carriers in different states then can be expressed by the

following rate equation system [1]:

$$\begin{aligned} \dot{n}_c &= \nu n - n_c(N-n)A - n_c n_h A_r \\ \dot{n} &= -\nu n + n_c(N-n)A \\ \dot{n}_h &= -n_c n_h A_r \end{aligned} \tag{1}$$

where the introduced terms are n_c, number of electrons in the conduction band; n, number of electrons in traps; n_h, number of holes in recombination centres; N, number of electron traps; ν, release rate for electrons from the traps; A, capture rate of electrons into traps; and A_r, recombination rate of electrons at the impurities.

From charge neutrality one gets $n_c + n = n_h$. It is usually assumed that (i) the number of electrons in the band is always small compared to the number of electrons in the traps ($n_c \ll n$) and (ii) the number of free electrons can be considered as quasi-stationary ($\dot{n}_c \ll \dot{n}$). Then equation system (1) reduces to

$$\dot{n} = \dot{n}_h = -\frac{\nu n^2}{n + R(N-n)} \tag{2}$$

where $R = A/A_r$. If retrapping is negligible ($R \ll n/(N-n)$), equation (2) describes first-order kinetics

$$\dot{n} = -\nu n \tag{3a}$$

whereas for the other extreme of dominating retrapping one expects second-order kinetics

$$\dot{n} = -\frac{\nu}{RN} n^2. \tag{3b}$$

For thermally activated processes the time dependence of ν is given by $\nu(E,t) = \nu_0 \exp(-E/kT(t))$, where the time dependence of the temperature $T(t)$ describes the applied heating procedure. In the present experiments it is given either by a linear ramp or a step-like curve.

The pre-exponential factor ν_0 poses problems. Typical values given in the literature differ by several orders of magnitude. If one single phonon is sufficient to release the electron, ν_0 should be given by $\nu_D \exp(S/k)$, where ν_D is of the order of the Debye frequency and S is the entropy associated with the trap (typically of the order of k). If, however, a multiphonon process is involved, ν_0 becomes energy dependent and is given by [18]

$$\nu_0(E) = \nu_D \exp(S/k) \exp(-\gamma E/E_D) \tag{4}$$

where ν_D is the Debye frequency, $E_D = h\nu_D$ the Debye energy and γ is of the order of unity. In the following a possible E dependence of ν_0 is ignored to improve the readability. All formulae derived below can be applied to multiphonon processes also, if $1/(kT)$ is replaced by $1/(kT) + \gamma/E_D$. Since in the final result the pre-exponential factor enters only logarithmically, all uncertainties mentioned are less serious than they may seem.

The observed thermoluminescence intensity $I(E,t)$ is proportional to $-\dot{n}$. Integrating equations (3*a*) and (3*b*) one gets for first-order kinetics

$$I(E,t) = n_0 \nu(E,t) \exp\left(-\int_0^t \nu(E,\tau)\, \mathrm{d}\tau\right) \tag{5a}$$

and for second-order kinetics

$$I(E,t) = \frac{n_0^2}{RN} \nu(E,t) \left(1 + \frac{n_0}{RN} \int_0^t \nu(E,\tau)\, \mathrm{d}\tau\right)^{-2} \tag{5b}$$

where n_0 is the number of trapped electrons at time $t = 0$.

The experiment has shown undoubtedly that a large number of traps with a broad distribution of activation energies is involved in the thermoluminescence process (figure 3). Therefore equations (5) have to be averaged over E to obtain the experimentally observed luminescence intensity

$$I(t) = \int I(E,t)n(E)\,\mathrm{d}E \tag{6}$$

where $n(E)$ is the activation energy distribution function.

At a given time always different traps with slightly different activation energies contribute simultaneously to the luminescence signal; therefore it is not possible to extract the order of kinetics from the time dependence. However, in the following we assume first-order kinetics. Arguments for this choice will be given in the next section.

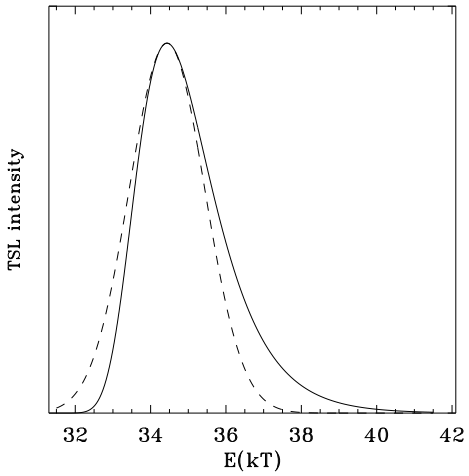

Figure 5. Solid line: thermoluminescence intensity for a fixed time $t = 500$ s after a single temperature step at time $t = 0$ (equation (11)). Broken line: Gaussian approximation of the maximum. For the calculation the Debye frequency $\nu_D = 1.8 \times 10^{12}$ s^{-1} of solid Ar [19] was used.

Figure 2(c) and figure 3 show that the width of the 16 K TSL peak is of the order of several kelvins. Thus one can conclude already without any calculation that the width of the distribution function $n(E)$ is of the same order as E. The same holds for the 23 K peak. Under these circumstances the integral (6) can be evaluated approximately. It is easily seen that $I(E,t)$ approaches zero in the limits $E \to 0$ and $E \to \infty$ and (for fixed t) has a maximum width of the order of kT. For the special case of a single temperature step this is illustrated in figure 5. This allows one to approximate $I(E,t)$ by a Gaussian function

$$I(E,t) = I(\overline{E},t)\exp\left[-(E-\overline{E})^2/(2\Delta^2)\right] \tag{7}$$

with a maximum at position $\overline{E}$ and a width of Δ. Inserting this Gaussian function into the integral (6) and assuming that the width of $n(E)$ is large compared to Δ, one gets

$$I(t) = (2\pi)^{1/2}\Delta I(\overline{E},t)n(\overline{E}). \tag{8}$$

The calculation of $I(\overline{E},t)$, $\overline{E}$ and Δ is performed in the appendix. The result is

$$I(t) = \frac{(2\pi)^{1/2}}{e} n_0 \alpha k \dot{T}\, n(\alpha kT) \tag{9}$$

where α is a solution of the transcendental equation

$$\alpha e^{\alpha} = \frac{\nu_0 T}{\dot{T}}. \tag{10}$$

Equation (9) constitutes the main result of this section. It shows that for a constant heating rate the thermoluminescence intensity as a function of T yields directly, up to the only weakly temperature dependent prefactor α, the trap energy distribution function $n(E)$. For a time dependent heating rate $I(t)$ is additionally modulated by $\dot{T}$. This modulation is responsible for the thermoluminescence flashes observed if the temperature is increased in a step-like way.

The $1/t$-dependence of the thermoluminescence intensity observed for step-like heating after each temperature step can also easily be understood. Assuming for the sake of simplicity that the temperature is raised one single step at time $t = 0$, one obtains from (5*a*)

$$I(E,t) = n_0 \nu_0 \exp\left(-\frac{E}{kT} - \nu_0 t e^{-E/(kT)}\right). \tag{11}$$

Inserting this expression into (6) and proceeding as above, one gets

$$I(t) = n_0 \frac{kT}{t}\left[1 - \exp(-\nu_0 t)\right]\, n[kT \ln(\nu_0 t)] \tag{12}$$

showing for times $t \gg 1/\nu_0$ the experimentally found $1/t$ behaviour (in fact for this case the calculation is considerably easier than that above, as $\overline{E}$ and the integral of $I(E,t)$ over E can be calculated exactly).

5. Conclusions

The experiments have shown that in the case of solid Ar electrons are released from an *intrinsic* trap with a maximum probability at $T_{\max} = 16$ K. Neglecting the weakly temperature dependent prefactor α in (9) the corresponding binding energy of the charge carriers in the traps can be calculated via

$$E = \alpha k T_{\max} \tag{13}$$

where α is a solution of (10). ν_0 can be estimated from (4) for multiphonon processes assuming for γ a typical value of unity. Thus one obtains in the case of solid Ar ($\nu_{\text{Debye}} = 1.8 \times 10^{12}$ s^{-1}) [19] $E \approx 36.5$ meV for the intrinsic electron trap.

For the TSC signal at 23 K parallel to the chemiluminescence of O_2 molecules one can conclude that here electrons are released from O^- ions acting as *extrinsic* traps. We were not able to decide whether the electrons are released before or during formation of the O_2 molecule. This is an important difference, because in the first case the extrinsic trap can be treated with exactly the same formalism as the intrinsic one, yielding a binding energy of $E \approx 49.8$ meV. This is orders of magnitudes smaller than the electron affinity of the free oxygen atom of 1.46 eV [20]. Thus even without knowledge of the exact interaction of the O^- ion with the host crystal this process seems improbable. In the other case the thermally stimulated process is the diffusion of oxygen atoms and $E = 49.8$ meV has to be interpreted as the migration enthalpy of O atoms or O^- ions in the Ar matrix.

A still open question is the structure of the intrinsic electron traps. Electron transport measurements [8] show that the transport is not limited by electron trapping, in a perfect crystal no intrinsic electron traps such as polarons seem to exist. However, defects in the crystal could serve as traps. It is known that x-ray irradiation of solid Ar produces a large number of Frenkel pairs, which can be detected by a macroscopic increase of the average

lattice constant [21]. Zero-order synchrotron irradiation should create defects similarly to x-rays. The radiative decay of the self-trapped excitons also releases enough energy for producing Frenkel pairs, which has been shown explicitly in the case of solid Xe using a selective excitation of excitons [22]. For the thermally activated recombination of Frenkel pairs activation enthalpies between 28 meV and 52 meV have been found in the case of solid Ar [21], which is exactly in the range of the binding energy for the intrinsic electron trap reported here. If one assumes, similarly to the discussion of the extrinsic electron traps above, that the Debye frequency is the dominating frequency for both the diffusion of interstitial atoms to the vacancies and the release of charges from traps, then the agreement of the binding energies is a strong argument that indeed Frenkel pairs serve as electron traps. The comparison of the total Au emission intensity during heating with the intensity of the same emission during exciton excitation yields a probability of 10^{-4}–10^{-3} per exciton for the production and population of the intrinsic traps in Ar.

In both models suggested for the intrinsic and extrinsic electron traps, respectively, the traps disappear upon the release of the electrons. Therefore a retrapping is impossible and the time dependence of the number of electrons in the traps has to be described by first-order kinetics.

Acknowledgments

This work was supported by the Bundesministerium für Forschung und Technologie of the Federal Republic of Germany. We would like to thank Dr W Schulze (Fritz-Haber-Institut Berlin) for giving us the opportunity to study our systems with their apparatus at BESSY, S Bach, L König and Dr Ch Jackschath for their help during the beamtimes at BESSY, and Professor H Ackermann and Dr R Dersch for helpful discussions especially in the beginning of our thermoluminescence studies.

Appendix

To derive the Gaussian approximation $I(E,t) = I(\overline{E},t)\exp\left[-(E-\overline{E})^2/(2\Delta^2)\right]$, equation (5*a*) is written as $I(E,t) = \exp(-g(E))$, with

$$g(E) = -\ln(n_0\nu_0) + \beta E + \nu_0 \int_\beta^\infty \mathrm{e}^{-\tilde{\beta}E}\frac{\mathrm{d}\tilde{\beta}}{|\dot{\beta}(\tilde{\beta})|} \tag{A1}$$

where the new variable $\beta = 1/(kT)$ was introduced. The position of the maximum $\overline{E}$ can be calculated from the zero of the first derivative and the width Δ from the second derivatives at the maximum $\overline{E}$. For the first and second derivatives one gets

$$\begin{aligned} g'(E) &= \beta - \nu_0 \int_\beta^\infty \tilde{\beta}\mathrm{e}^{-\tilde{\beta}E}\frac{\mathrm{d}\tilde{\beta}}{|\dot{\beta}(\tilde{\beta})|} \\ g''(E) &= \nu_0 \int_\beta^\infty \tilde{\beta}^2\mathrm{e}^{-\tilde{\beta}E}\frac{\mathrm{d}\tilde{\beta}}{|\dot{\beta}(\tilde{\beta})|}. \end{aligned} \tag{A2}$$

Because of the exponential $\exp(-\tilde{\beta}E)$ the main contributions to the integrals come from $\tilde{\beta}$ values close to β. Under this approximation the integrations can be performed and yield

$$\begin{aligned} g(E) &= -\ln(n_0\nu_0) + \beta E + \frac{\nu_0}{|\dot{\beta}|E}\,\mathrm{e}^{-\beta E} \\ g'(E) &= \beta\left(1 - \frac{\nu_0}{|\dot{\beta}|E}\,\mathrm{e}^{-\beta E}\right) \end{aligned} \tag{A3}$$

$$g''(E) = \beta^2 \frac{\nu_0}{|\dot{\beta}|E}\ \mathrm{e}^{-\beta E}.$$

$\overline{E}$ is obtained from $g'(\overline{E}) = 0$, whence follows

$$\frac{\nu_0}{|\dot{\beta}|\overline{E}}\ \mathrm{e}^{-\beta\overline{E}} = 1. \tag{A4}$$

Equation (10) follows directly from (A4). Inserting (A4) into (A3) for $g(E)$ and $g''(E)$ one gets

$$\begin{aligned} g(\overline{E}) &= -\ln I(\overline{E}, t) = -\ln(n_0|\dot{\beta}|\overline{E}) + 1 \\ g''(\overline{E}) &= \Delta^{-2} = \beta^2 \end{aligned} \tag{A5}$$

whence follows

$$I(\overline{E}, t) = n_0|\dot{T}|\overline{E}/\mathrm{e}kT^2 \tag{A6}$$

$$\Delta = kT. \tag{A7}$$

References

[1] McKeever S W S 1985 *Thermoluminescence of Solids* (Cambridge: Cambridge University Press) p 40
[2] Fajardo M E and Apkarian V A 1988 *J. Chem. Phys.* **89** 4124
[3] Danilychev A V and Apkarian V A 1993 *J. Chem. Phys.* **99** 8617
[4] Dersch R, Herkert B, Witt M, Stöckmann H-J and Ackermann H 1990 *Z. Phys.* B **80** 39
[5] Kirm M and Niedrais H 1994 *J. Lumin.* **60&61** 611
[6] Steinmetz N, Menges H, Dutzi J, von Löhneysen H and Goldacker W 1989 *Phys. Rev.* B **39** 2838
[7] Schrimpf A, Rosendahl R, Bornemann T, Stöckmann H-J, Faller F and Manceron L 1992 *J. Chem. Phys.* **96** 7992
[8] Spear W E and Le Comber P G 1977 *Rare Gas Solids* vol 2, ed M L Klein and J A Venables (London: Academic) p 1120
[9] Umehara M 1986 *Phys. Rev.* B **33** 4237
[10] Umehara M 1986 *Phys. Rev.* B **33** 4245
[11] Ralls K M, Courtney T H and Wulff J 1976 *Introduction to Materials Science and Engineering* (New York: Wiley) p 55
[12] Herkert B, Schrimpf A, Göttsche K, Bornemann T and Stöckmann H-J 1995 *Phys. Rev.* B **51** 15 763
[13] Schrimpf A 1995 *Excitonic Processes in Condensed Matter* ed J Singh *Proc. SPIE* **2362** 592
[14] Herkert B, Schrimpf A, Göttsche K, Bornemann T, Brüning R and Stöckmann H-J 1994 *J. Lumin.* **60&61** 768
[15] Saile V 1980 *Appl. Opt.* **19** 4115
[16] Bernstorff S and Saile V 1986 *Opt. Commun.* **58** 181
[17] Schuberth E and Creuzburg M 1978 *Phys. Status Solidi* b **90** 189
[18] Hayes W and Stoneham A M 1985 *Defects and Defect Processes in Nonmetallic Solids* (New York: Wiley) p 209
[19] Korpuin P and Lüscher E 1977 *Rare Gas Solids* vol 2, ed M L Klein and J A Venables (London: Academic) p 763
[20] Smirnov B M 1981 *Negative Ions* (New York: McGraw-Hill)
[21] Balzer R and Giersberg E-J 1980 *Phys. Status Solidi* a **57** K141
[22] Varding D, Becker J, Frankenstein L, Peters B, Runne M, Schröder A and Zimmerer G 1993 *Low Temp. Phys.* **19** 427
[23] Schrittenlacher W and Kolb D M 1984 *Ber. Bunsenges. Phys. Chem.* **88** 492